SOLAR WIND MODEL IN THE SWMF.

Igor V. Sokolov[1], Richard E. Mullinix[2], Aleksandre Taktakishvili[2], Doga Can Su Ozturk[1], Judit Szente[1], Anna Chulaki[2], Meng Jin[3], Ward B. Manchester[1], Bart van der Holst[1] and Tamas Gombosi[1]

1. CLaSP, University of Michigan, Ann Arbor MI
2. CCMC, Goddard Space Flight Center, Greenbelt MD
3. Lockheed Martin Solar and Astrophysics Lab,Palo Alto CA

+Thanks to Maria M. Kuznetsova and Spiro Antiochos
+Special thanks to Nykyri, Heidi K, who explained me that some participants do not speak Russian.

April, 04, 2016. Isradynamics 2016: Dynamical Processes in Space Plasma, Isrotel, Ein Bokek, Dead Sea, Izrael.

Solar Wind Models (from prophet Moyses to Ofer Cohen)

- **Solar wind is the plasma state within the heliosphere, say , at 15-30 R_S, <R < 1-3 AU.**
- **Features:**
  - Windy (outward motional speed dominates over all other characteristic speed: thermal, Alfven ets)
  - Bimodal structure: fast (and rarefied, and electrons stay cold on the way – low charge states of oxigen) wind and slow (and intermittent, and dense and electrons are hot somewhere on the way: higher charge states of oxygen)
- **Very easy to simulate:**
  - Purely super"sonic" outward propagating flow, therefore, the BC at 15-30R_S well-poses the problem mathematically.
  - Conveniently large time step (5-10 minutes).
  - Good WSA semi-empirical model to derive the BC at 5-30R_S
  - A possibility to use Bernoulli integral to relate the observed magnetogram to asymptotic properties of the solar wind at 1 AU (Ofer Cohen et al,2007-2008)

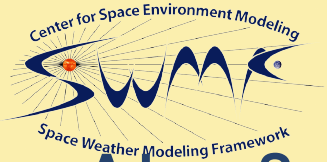

Why Field-Line-Threaded?

- A Low Solar Corona is a key element of a global computational model for the solar atmosphere and inner heliosphere. This is the place from which the solar wind originates and the place where the heat flux from the hotter Solar Corona to the colder chromosphere controls the corona base plasma parameters. Within our AWSoM model including the Alfven Wave Turbulence as the only heating agent, the Low Solar Corona is the domain to set the boundary condition for the Poynting flux as well as the wave reflection from the transition region.
- To resolve the transition region, the spatial resolution should be about 1 Mm. The large fraction of the computational resources should be devoted to simulate this region directly. A tiny grid size results in a severe restriction on the time step of the time accurate (non-steady-state) simulations, making unfeasible the real-time modeling.
- Field-Line-Threaded approach allows us to both save computational resources and avoid severe limitation on the time step. Following the idea of the ‘radiation energy balance’ boundary condition (Lionello et al. 2009 and papers cited therein), we essentially extend its capability.

Governing Equations of the 3D AWSoM

$$\frac{\partial \rho}{\partial t} + \nabla \cdot (\rho \mathbf{u}) = 0$$

$$\frac{\partial \rho \mathbf{u}}{\partial t} + \nabla \cdot (\rho \mathbf{u}\mathbf{u} + P + \frac{B^2}{2\mu} - \frac{\mathbf{B}\mathbf{B}}{\mu} + \frac{w_- + w_+}{2}) = -\frac{GM_S \rho \mathbf{r}}{r^3}$$

$$\frac{\partial}{\partial t}\left(\frac{P}{\gamma - 1} + \frac{\rho u^2}{2} + \frac{B^2}{2\mu}\right) + \nabla \cdot \left[\mathbf{u}\left(\frac{\gamma P}{\gamma - 1} + \frac{\rho u^2}{2} + \frac{B^2}{2\mu}\right) - \frac{\mathbf{B}(\mathbf{u} \cdot \mathbf{B})}{\mu}\right] =$$

$$= (\mathbf{u} \cdot \nabla)\frac{w_- + w_+}{2} + \Gamma_- w_- + \Gamma_+ w_+ + \nabla \cdot (\frac{\mathbf{B}\mathbf{B}}{B^2} \kappa \cdot \nabla T_e) - Q_{rad}$$

$$\frac{\partial w_\pm}{\partial t} + \nabla \cdot [(\mathbf{u} \pm \mathbf{V}_A) w_\pm] + \frac{w_\pm}{2}(\nabla \cdot \mathbf{u}) = \mp R\sqrt{w_- w_+} - \Gamma_\pm w_\pm$$

$$R = \min\left\{\sqrt{(\mathbf{b} \cdot [\nabla \times \mathbf{u}])^2 + [(\mathbf{V}_A \cdot \nabla)\log V_A]^2}, \max(\Gamma_\pm)\right\} \times$$

$$\left[\max(1 - 2\sqrt{\frac{w_-}{w_+}}, 0) - \max(1 - 2\sqrt{\frac{w_+}{w_-}}, 0)\right],$$

$$\Gamma_\pm = \frac{1}{L_\perp}\sqrt{\frac{w_\mp}{\rho}}, \quad 50[km \cdot \sqrt{T}] < L_\perp \sqrt{B} < 200[km \cdot \sqrt{T}]$$

Solar Wind Model in the SWMF: current development

- **Why development? Disadvantages of the semi-empirical models:**
  - There could be almost perfect matching of empirical coefficients for the most of Carrington rotations (but what can we say today about the CR 2175 which is not over yet?).
  - Lack of physics and lack of belief. We do not understand, how at very small altitudes (the charge states which distinguish slow and fast solar wind may freeze up at 1.2R_S of heliocentric distance). And we cannot agree that we should believe in some sort karma and not to care about the reasons, but benefit from the consequences.
- **There is an interest to physics-based model, hence, started at on top of the TR or even on top of chromosphere. AWSoM model: Alfven wave turbulence as the only source of coronal heating and solar wind acceleration AND the model starts from chromosphere.**
- **In this case we successfully arrive at computationally intense problem which we solve using the threaded-field-line model AWSoM_R model (AWSoM model working in Real time).**
- **Some tools allowing to simulate ongoing CMEs (STEREO CAT, EEGGL**

SWMF/AWSoM Model

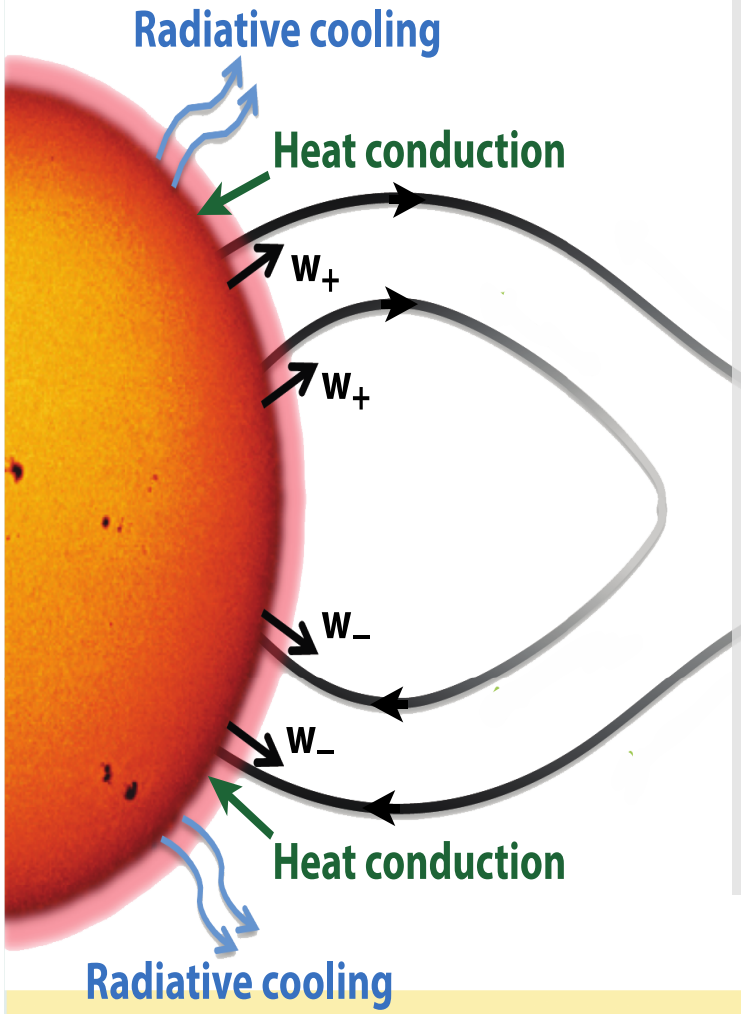

Heat conduction: Spitzer ($r<5R_s$) + Hollweg ($r>5R_s$)
Radiative cooling from CHIANTI
Wave pressure gradient accelerates and heats
Two (T_i, T_e) or three ($T_{i\parallel}$, $T_{i\perp}$, T_e) temperatures
Turbulent energy transport along field lines:

$$\frac{\partial w_\pm}{\partial t} + \nabla\cdot\left[\left(\mathbf{u}\pm\mathbf{V}_A\right)w_\pm\right] + \frac{w_\pm}{2}\left(\nabla\cdot\mathbf{u}\right) = \mp\mathcal{R}\sqrt{w_- w_+} - \Gamma_\pm w_\pm$$

$$\Gamma_\pm = \frac{2}{L_\perp}\sqrt{\frac{w_\mp}{\rho}} \qquad L_\perp\sqrt{B} = 150\ \mathrm{km}\sqrt{T} \qquad (\Pi/\mathcal{B}) = 1.1\times10^6\ \mathrm{Wm^{-2}T^{-1}}$$

$$\mathcal{R} = \min\{\mathcal{R}_{imb}, \max\left[\Gamma_\pm\right]\}\begin{cases}\left(1-2\sqrt{\frac{w_-}{w_+}}\right) & w_+ \geq 4w_- \\ 0 & \frac{1}{4}w_- < w_+ < 4w_- \\ \left(2\sqrt{\frac{w_-}{w_+}}-1\right) & w_+ \leq \frac{1}{4}w_-\end{cases}$$

$$\mathcal{R}_{imb} = \sqrt{\left[\left(\mathbf{V}_A\cdot\nabla\right)\log V_A\right]^2 + \left[\frac{\mathbf{B}}{B}\cdot\left(\nabla\times\mathbf{u}\right)\right]^2}$$

Sokolov et al., ApJ, **764**, 23 (2013).
van der Holst et al., ApJ, **782**, 81 (2014).

Alfvén Wave Turbulence

- **Wave energy densities of counter-propagating transverse Alfvén waves parallel (+) and anti-parallel (-) to magnetic field:**

energy reduction in expanding flow

wave dissipation

$$\frac{\partial w_\pm}{\partial t} + \nabla\cdot\left[\left(\mathbf{u} \pm \mathbf{V}_A\right) w_\pm\right] + \frac{w_\pm}{2}(\nabla\cdot\mathbf{u}) = \mp\mathcal{R}\sqrt{w_- w_+} - \Gamma_\pm w_\pm$$

Alfvén wave advection

wave reflection

$$\mathcal{R} = \min\left[\sqrt{[(\mathbf{V}_A\cdot\nabla)\log V_A]^2 + (\mathbf{b}\cdot[\nabla\times\mathbf{u}])^2}, \max(\Gamma_\pm)\right]\begin{cases} \left(1-2\sqrt{\dfrac{w_-}{w_+}}\right) & \text{if} \quad 4w_- \le w_+ \\ 0 & \text{if} \quad \frac{1}{4}w_- \le w_+ \le 4w_- \\ \left(2\sqrt{\dfrac{w_+}{w_-}}-1\right) & \text{if} \quad 4w_+ \le w_- \end{cases}$$

- **Phenomenological wave dissipation (Dmitruk et al., 2002):** $\Gamma_\pm = \dfrac{2}{L_\perp}\sqrt{\dfrac{w_\mp}{\rho}}$
- **Similar to Hollweg (1986), we use a simple scaling law for the transverse correlation length** $L_\perp\sqrt{B} = 150\,\mathrm{km}\sqrt{\mathrm{T}}$
- **Poynting flux of outward propagating turbulence:** $(\Pi/B) = 1.1\times10^6\,\mathrm{Wm^{-2}T^{-1}}$

From AWSoM to AWSoM_R. Why Field-Line-Threaded?

- A Low Solar Corona is a key element of a global computational model for the solar atmosphere and inner heliosphere. This is the place from which the solar wind originates and the place where the heat flux from the hotter Solar Corona to the colder chromosphere controls the corona base plasma parameters. Within our AWSoM model including the Alfven Wave Turbulence as the only heating agent, the Low Solar Corona is the domain to set the boundary condition for the Poynting flux as well as the wave reflection from the transition region.
- To resolve the transition region, the spatial resolution should be about 1 Mm. The large fraction of the computational resources should be devoted to simulate this region directly. A tiny grid size results in a severe restriction on the time step of the time accurate (non-steady-state) simulations, making unfeasible the real-time modeling.
- Field-Line-Threaded approach allows us to both save computational resources and avoid severe limitation on the time step. Following the idea of the 'radiation energy balance' boundary condition (Lionello et al. 2009 and papers cited therein), we essentially extend its capability.

Computational Grid: AWSoM

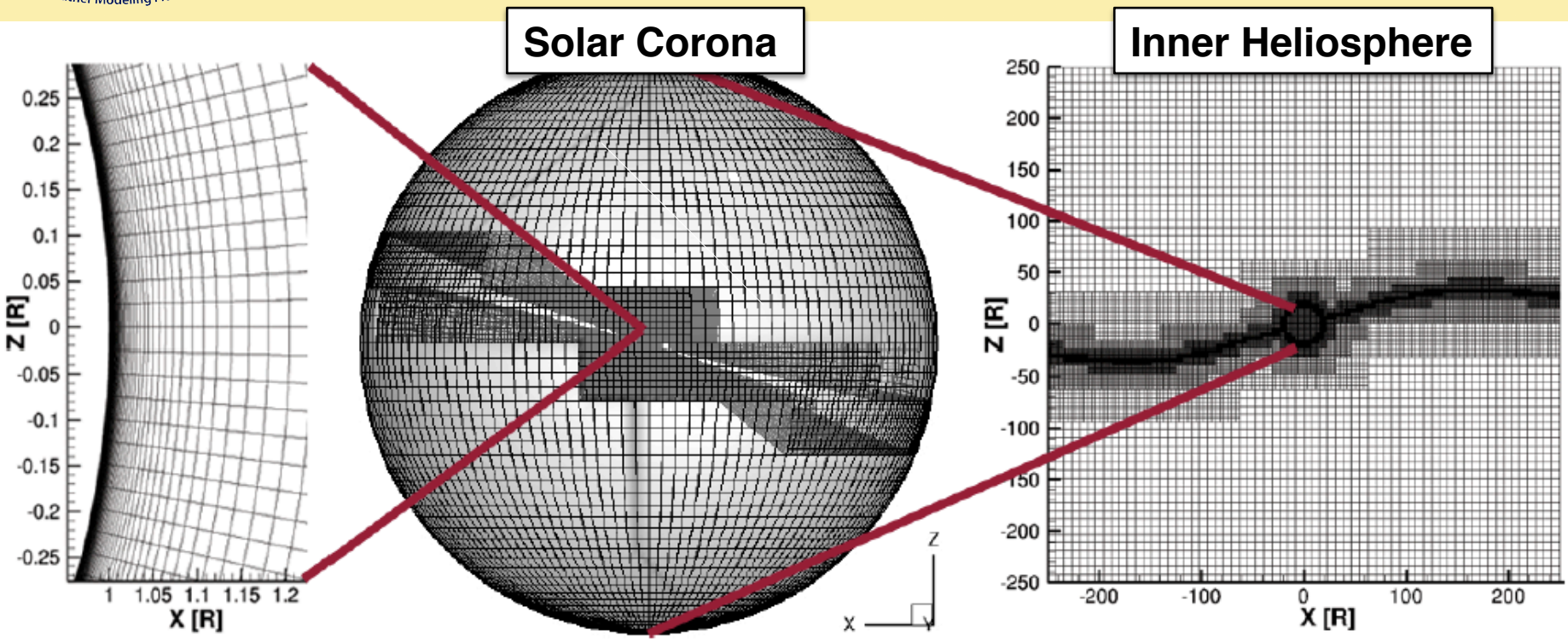

- Significant grid stretching to grid resolve the upper chromosphere and transition region in addition to artificial transition region broadening (Lionello et al. 2009, Sokolov et al. 2013)

AWSoM-R: Upshift the Low Boundary

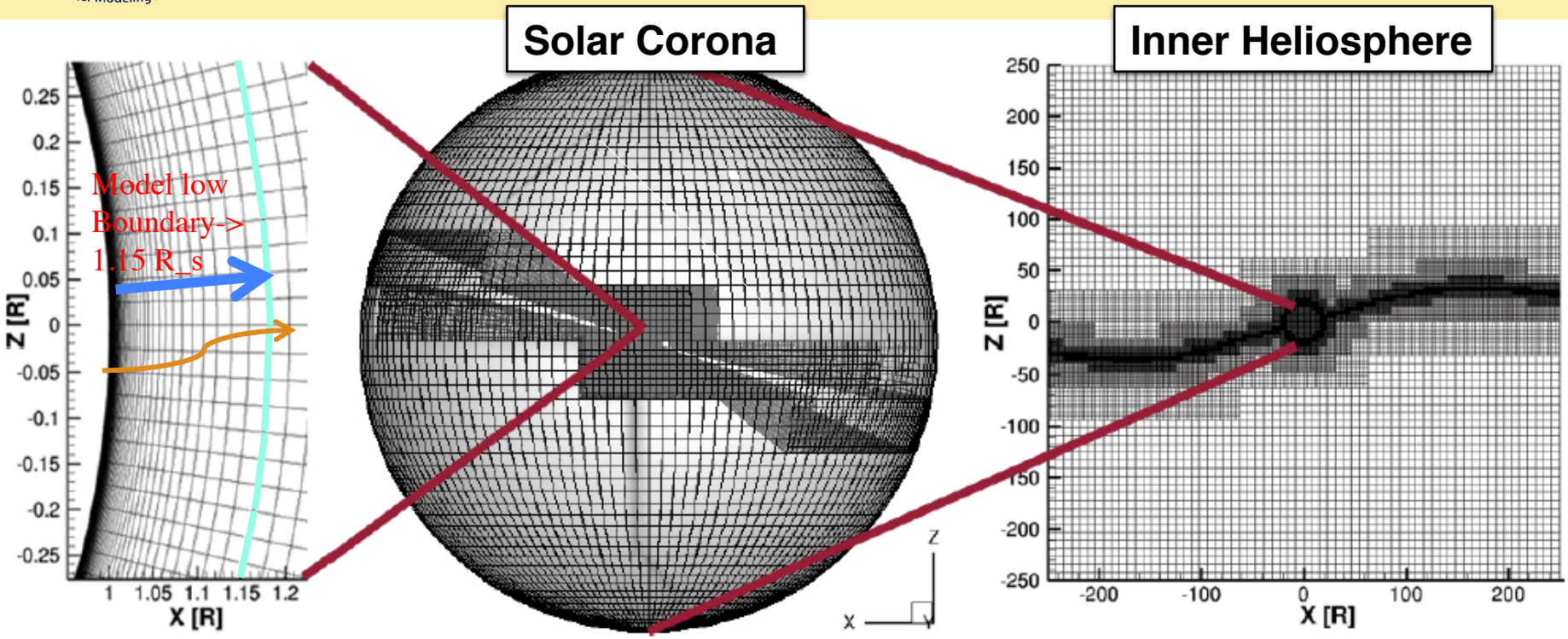

- We use the lower boundary of the model at R=1.15Rs
- All resources spent to cover the low corona within the AWSoM model are saved in the AWSoM-R (significant speedup)

Apply 1D thread solution.

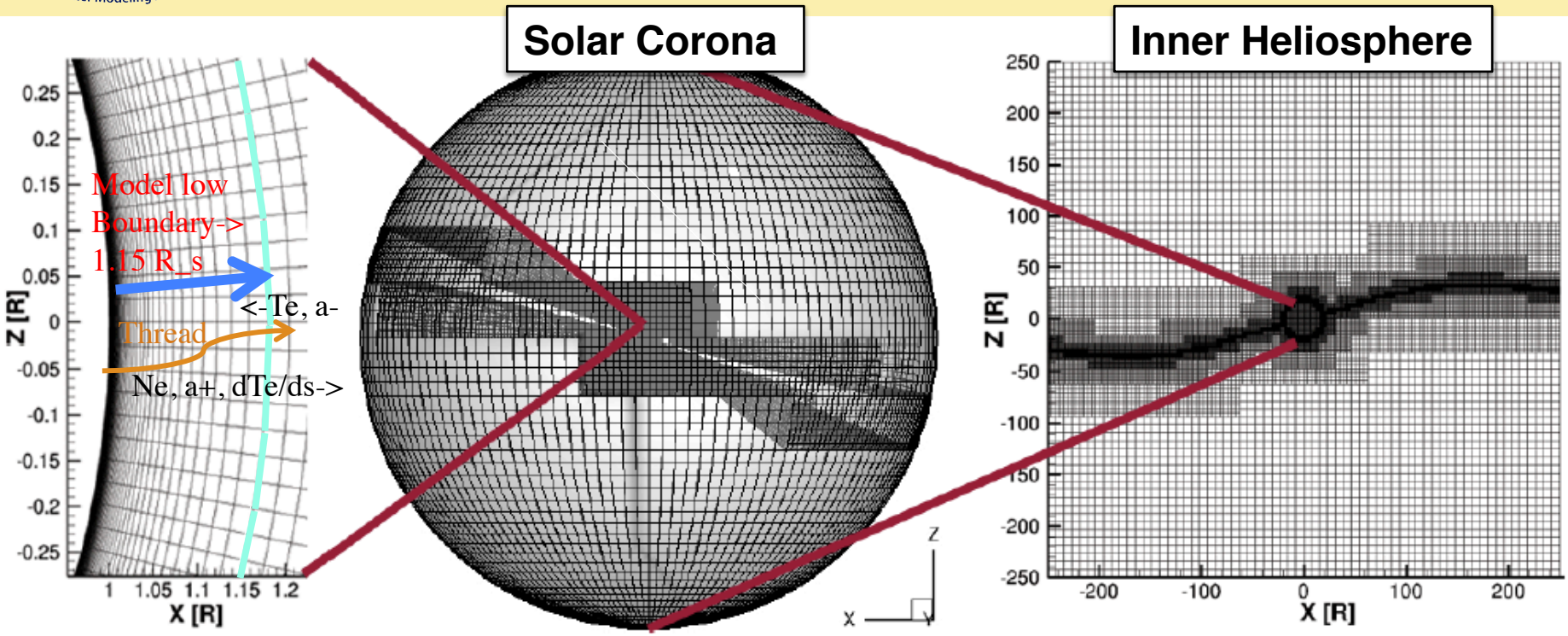

- We apply 1D thread solution to bridge the AWSoM-R model to the chromosphere through the TR.

Threaded Field Line Model

- Recognize that between $1R_s$ and R_b=$1.05R_s$ **u || B** and $u \ll V_{slow}, V_A, V_{fast}$
- Inner boundary of AWS☼M-R is at 1.05Rs
- Each boundary cell center is connected to the upper chromosphere by a magnetic field line
- An important point which we often miss in out explanations. We always split the coronal field for a potential and not potential parts and the observed magnetogram is applied to the potential part within the PFSSM. In AWSoM the non-potential field vabishes at R=R_S. In AWSoM_R the not-potential field vanishes within the range, R_S<R<R_b.
- Quasi-steady-state mass, momentum and energy transport is solved along the connecting field line (**1D** equations!)

$$\frac{\rho}{B} u_{\parallel} = \text{const} \qquad \frac{d}{ds}\left[n\, k_B \left(T_e + T_i\right) + \frac{w_+ + w_-}{2} \right] = -\rho \frac{d}{ds}\left(\frac{G\, M_\odot}{r} \right)$$

$$B \frac{d}{ds}\left[\frac{\rho}{B} u_{\parallel} \left(\frac{5 k_B \left(T_e + T_i\right)}{2 m_p} - \frac{G\, M_\odot}{r} \right) + \frac{w_+ - w_-}{\sqrt{\mu_0 \rho}} - \frac{\kappa_0 T_e^{5/2}}{B} \frac{dT_e}{ds} \right] = -n^2 \Lambda\left(T_e\right)$$

$$\nabla \cdot \left[\left(\mathbf{u} \pm \mathbf{V}_{\mathrm{A}} \right) w_{\pm} \right] + \frac{w_{\pm}}{2} \left(\nabla \cdot \mathbf{u} \right) = \mp \mathcal{R} \sqrt{w_- w_+} - \Gamma_{\pm} w_{\pm}$$

Wave Energy Transport in TFL Model

- Energy transport

$$\nabla \cdot \left[\left(\mathbf{u} \pm \mathbf{V}_\mathrm{A} \right) w_\pm \right] + \frac{w_\pm}{2} \left(\nabla \cdot \mathbf{u} \right) = \mp \mathcal{R} \sqrt{w_- w_+} - \Gamma_\pm w_\pm$$

- In the upper chromosphere (near lower boundary) $V_A >> u$ and all terms containing **u** can be neglected
- Assuming that near the chromosphere the Poynting flux (S_A) to magnetic field ratio is constant we can introduce a new dimensionless variable ($a_\pm$)

$$w_\pm = \frac{S_\mathrm{A}}{B} \sqrt{\mu_0 \rho}\, a_\pm^2$$

- Now the wave equation near the lower boundary is

$$\pm 2 V_\mathrm{A} \frac{da_\pm}{ds} = \mp \mathcal{R}\, a_\mp - \Gamma_\pm\, a_\pm^2$$

- Boundary condition at chromospheric boundary
  - Dimensionless amplitude is unity for outgoing wave
  - Dimensionless amplitude has zero gradient for incoming wave

Comparison of AWS☼M & AWS☼M-R

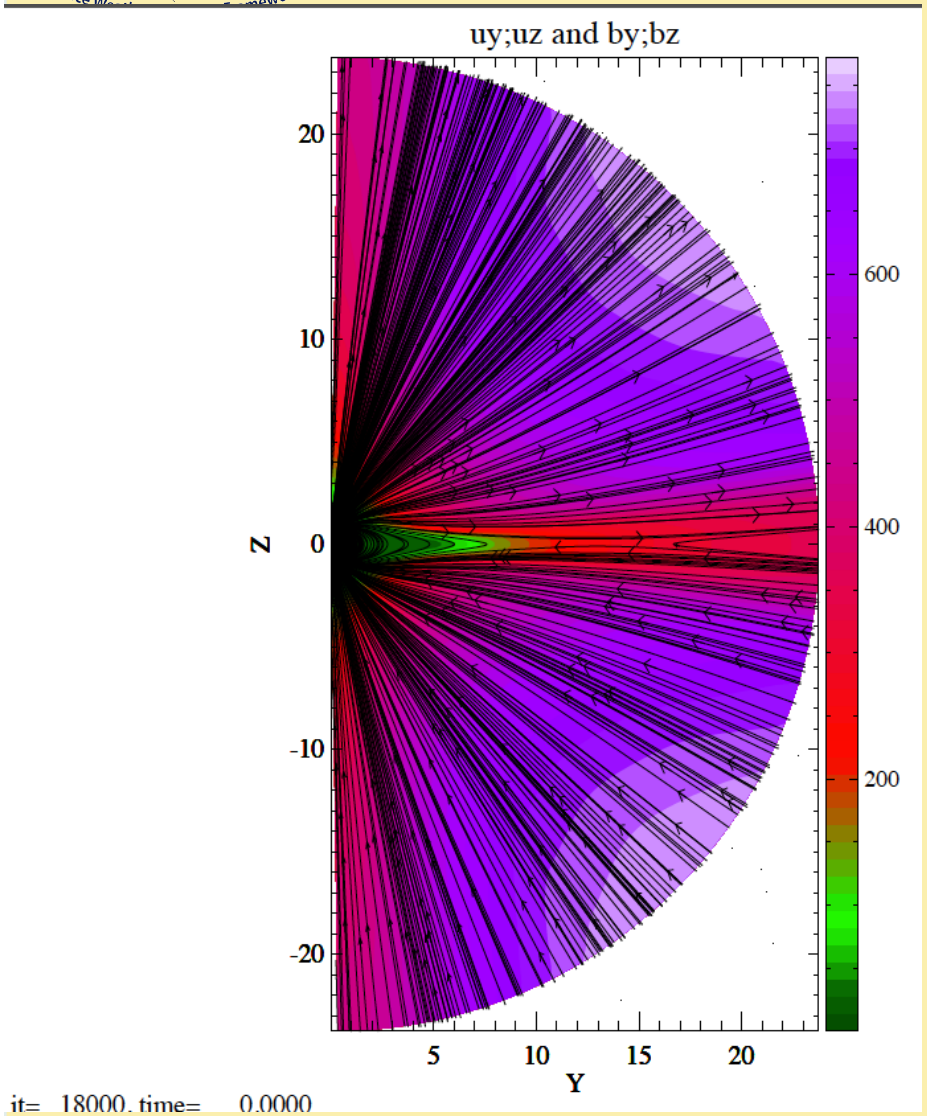

Dipole with AWSOM

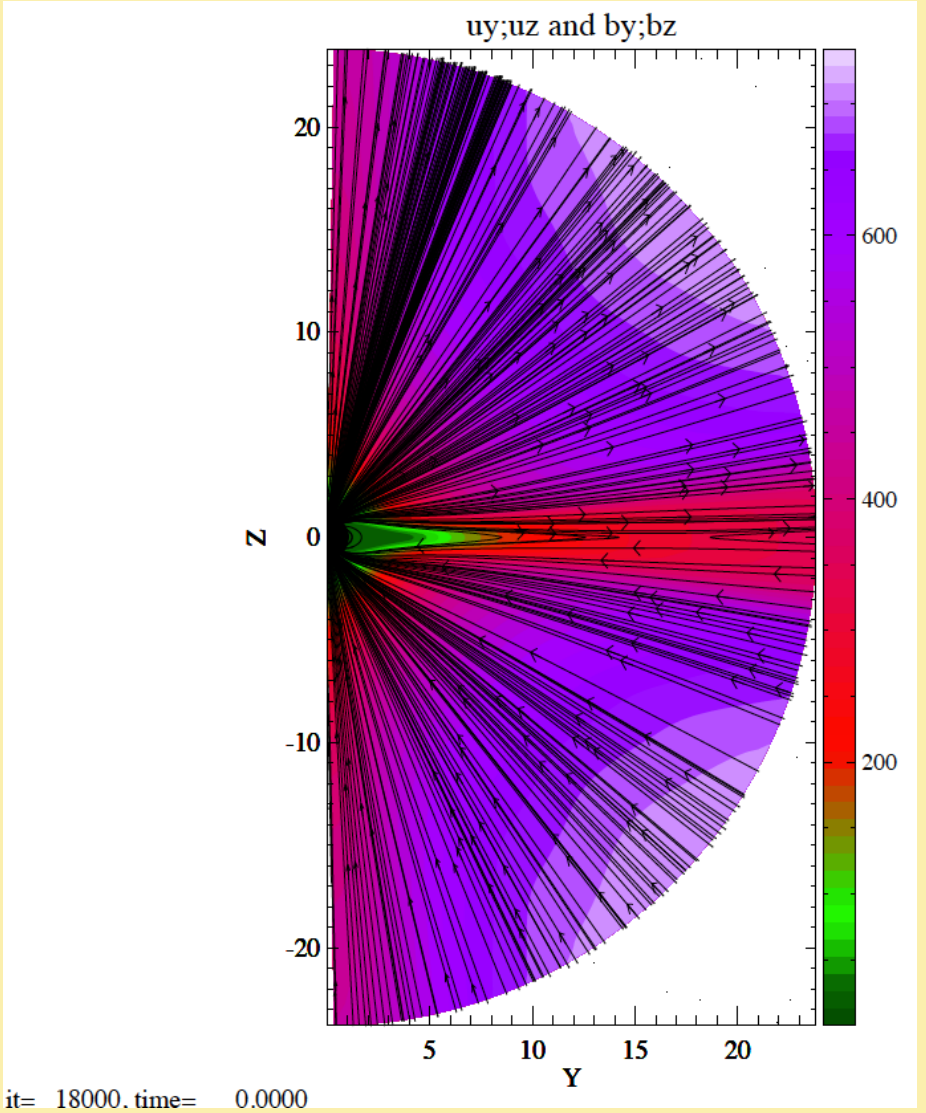

Dipole with AWSOM-R

Comparison of AWSOM-R & AWSOM-R

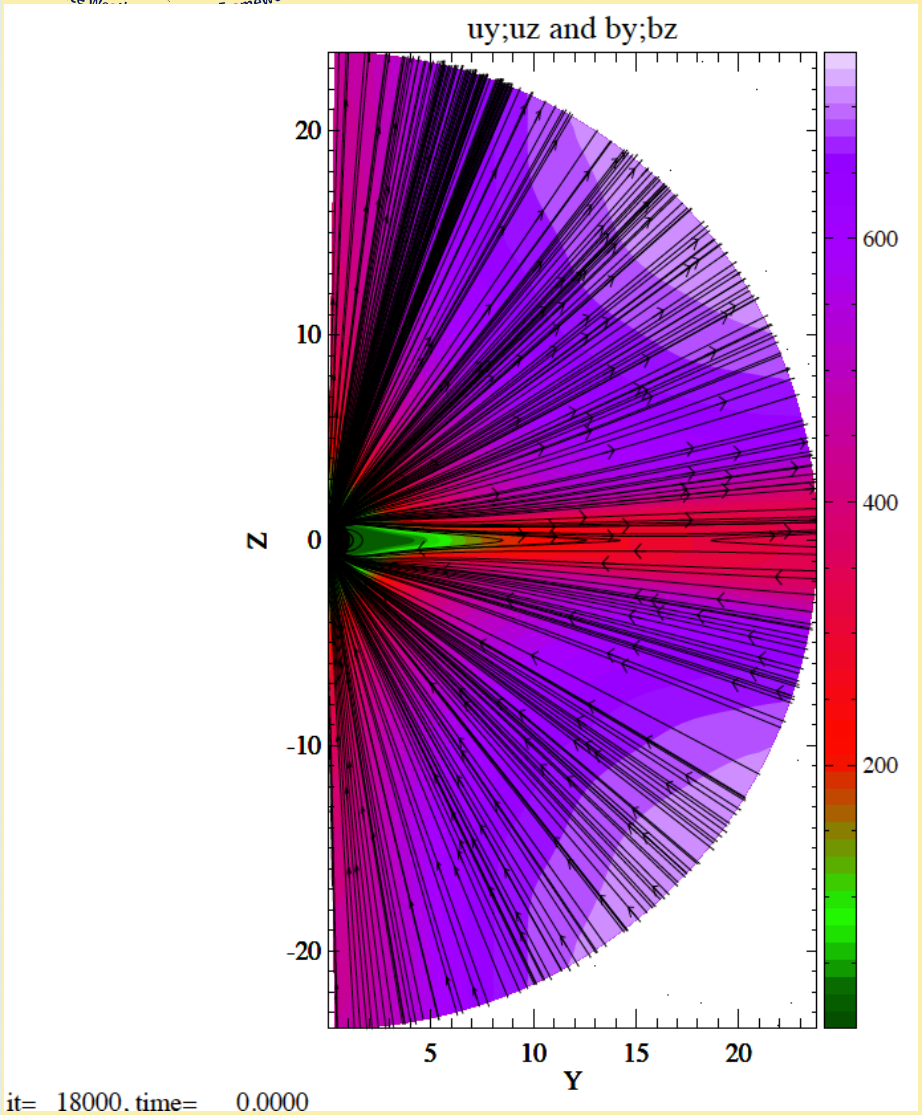

Dipole with AWSOM-R, low boundary at 1.05Rs

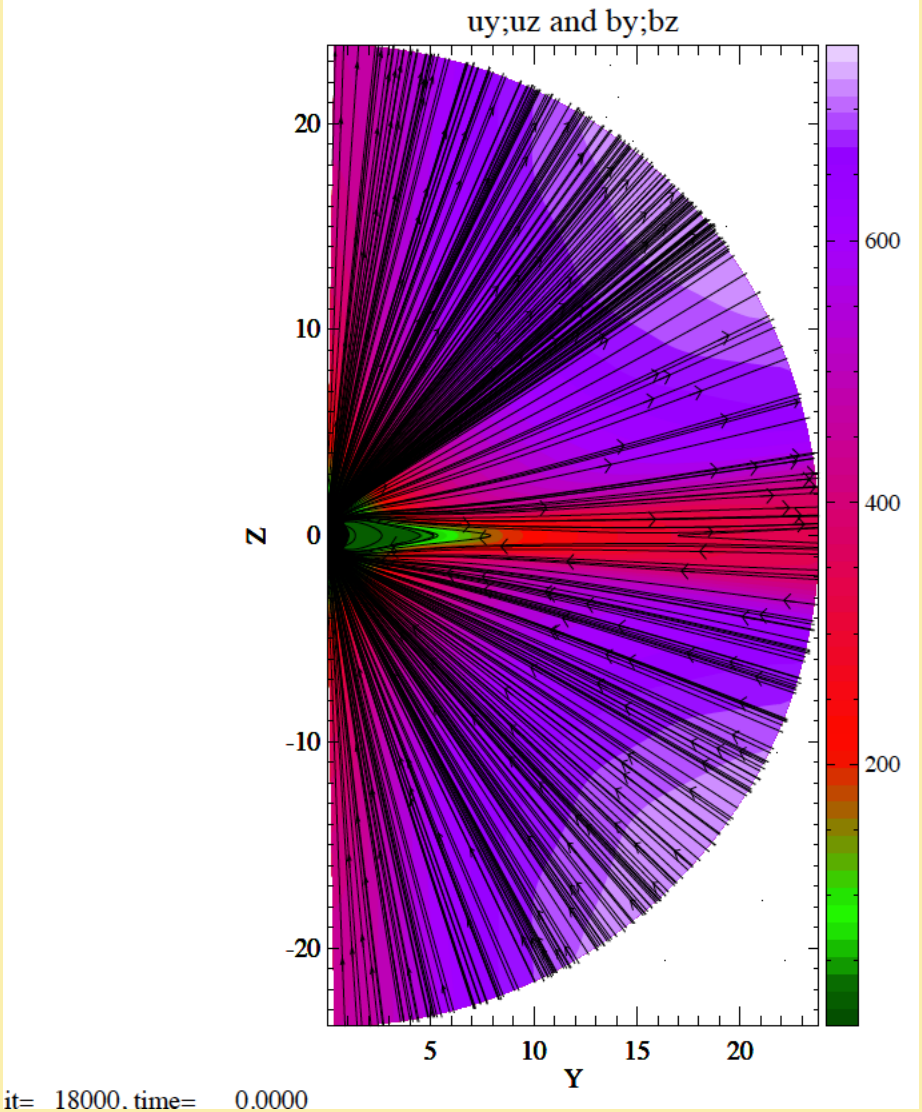

Dipole with AWSOM-R, low boundary at 1.10Rs

Judit Szente's Result for the Bi-modal solar wind structure from non-

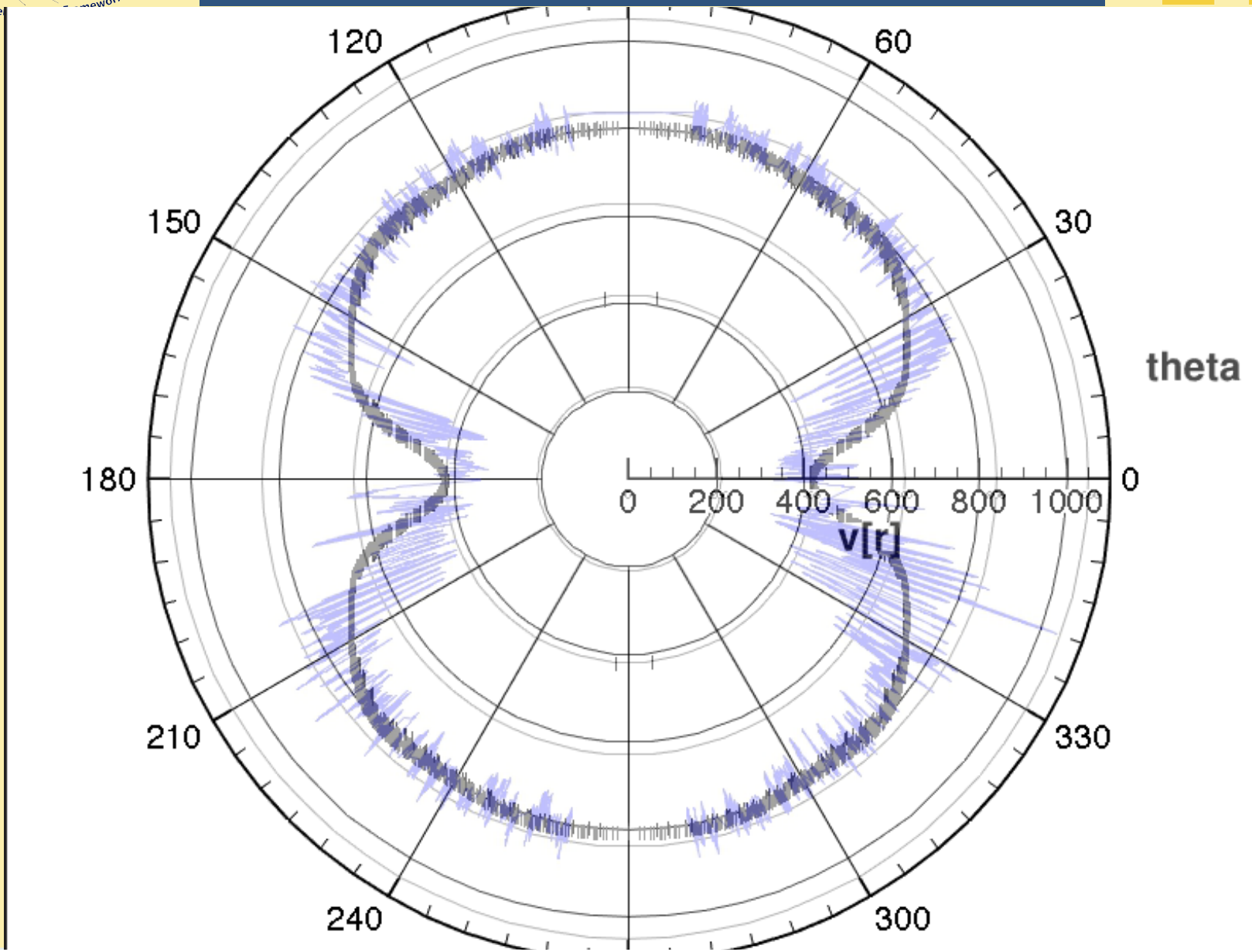

Reproduction of the solar wind observations at 1 AU

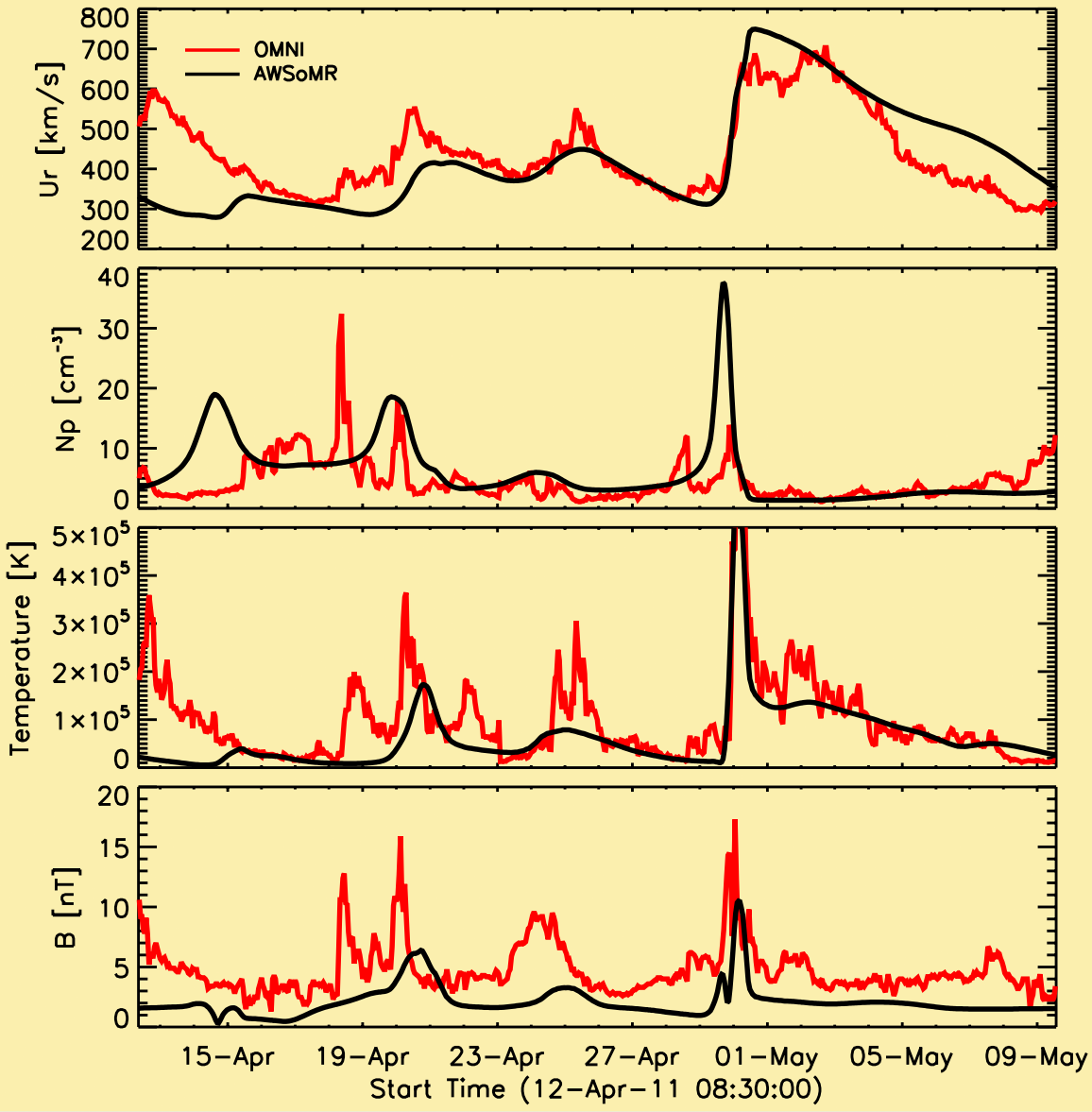

Intermittent plasmoid formation in a slow solar wind.

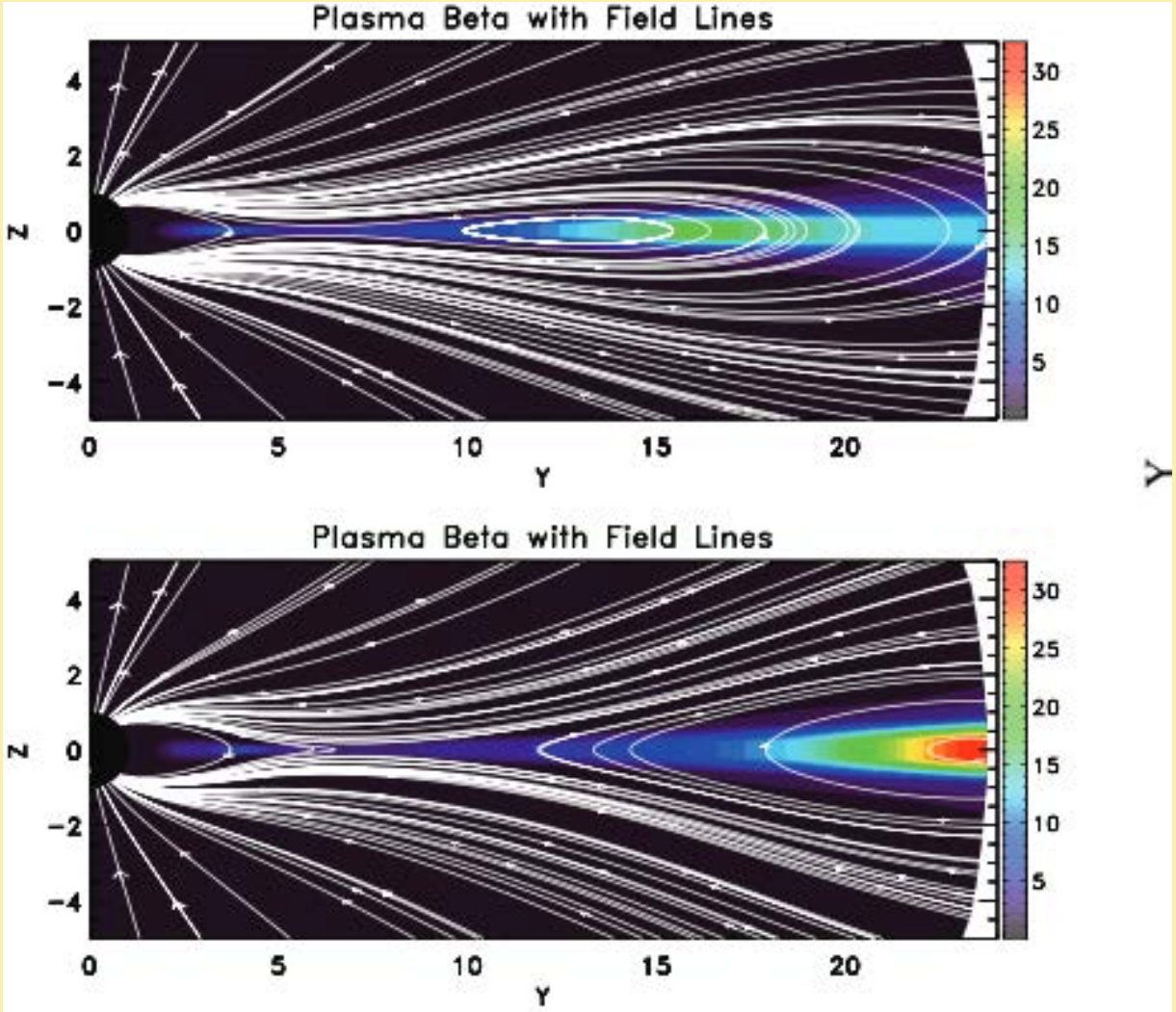

Figure - 4: The snapshots of the plasma beta and field lines at t1 = 3d14h40m (top) and t2 = 3d21h20m (bottom)

Conclusion about AWSoM vs AWSoM-R

Transients in the Solar Wind and Their Simulation in Real Time

- We present and demonstrate a new tool, EEGGL (Eruptive Event Generator using Gibson-Low configuration) for simulating CMEs Coronal Mass Ejections).
- CMEs are among the most significant space weather events, producing the radiation hazards (via the diffuse shock acceleration of the Solar Energetic Particles – SEPs), the interplanetary shock waves as well as the geomagnetic activity doe to the drastic changes of the interplanetary magnetic field within the "magnetic clouds" ("flux ropes"). Some of these effects may be efficiently simulated using the "cone model", which is employed in the real-time simulations of the ongoing CMEs at the NASA-Goddard Space Flight Center. The cone model provides a capability to predict the location, time, width and shape of the hydrodynamic perturbation in the upper solar corona (at ~0.1 AU), which can be used to drive the heliospheric simulation (with the ENLIL code, for example). At the same time the magnetic field orientation in this perturbation is uncertain within the cone model, which limits the capability of the geomagnetic activity forecast.

Eruptive Event Generator (Gibson-Low): EEGGL

- The new EEGGL tool recently developed at the Goddard Space Flight Center in collaboration with the University of Michigan provides a new capability for both evaluating the magnetic field configuration resulting from the CME and tracing the CME through the solar corona. In this way not only the capability to simulate the magnetic field evolution at 1 AU may be achieved, but the also the more extensive comparison with the CME observations in the solar corona may be achieved.
- Based on the magnetogram and evaluation of the CME initial location and speed, the user may choose the active region from which the CME originates and then the EEGGL tools provides the parameters of the Gibson-Low magnetic configuration to parameterize the CME. The recommended parameters may be used then to drive the CME propagation from the low solar corona to 1 AU using the global code for simulating the solar corona and inner heliosphere. The Community Coordinated Modeling Center (CCMC) provides the capability for CME runs-on-request, to the heliophysics community.

Demo for CME 2012-07-12

- We demonstrate how the new tools are used to simulate a halo CME 2012-07-12 (https://kauai.ccmc.gsfc.nasa.gov/DONKI/view/CME/14/1)

The List of CME Analysis already entered:

Event Type	Catalog	Data Level	Prime?	Long	Lat	Speed	Type	Half Width	Time 21.5	Note	WSA-ENLIL+Cone Result(s)	Submitted By
CME Analysis	SWRC_CATALOG	0	true	6.0	-13.0	1300.0	O	65.0	2012-07-12T19:29Z	remeasured using the GCS model	Not modeled	Leila Mays on 2015-06-01T19:02Z
CME Analysis	SWRC_CATALOG	0	false	-6.0	-17.0	1400.0	O	70.0	2012-07-12T19:35Z		1: Result 1 (2.0 AU) Earth = 2012-07-14T10:20Z (PE: -7.1 h) Mars = 2012-07-16T00:55Z MESSENGER = 2012-07-13T10:04Z Spitzer = 2012-07-14T13:56Z	Leila Mays on 2013-07-11T21:36Z
CME Analysis	SWRC_CATALOG	0	false	6.0	-9.0	1480.0	O	75.0	2012-07-12T19:31Z		1: Result 1 (2.0 AU) Earth = 2012-07-14T09:17Z (PE: -8.2 h) Mars = 2012-07-16T05:07Z MESSENGER = 2012-07-13T09:59Z Spitzer = 2012-07-14T15:06Z	Anthony Pritchard on 2013-08-08T20:48Z

StereoCAT is used to find CME Speed

- StereoCAT (http://ccmc.gsfc.nasa.gov/analysis/stereo/) is developed at the CCMC. By tracing the CME front, we find CME Speed=1300km/s.

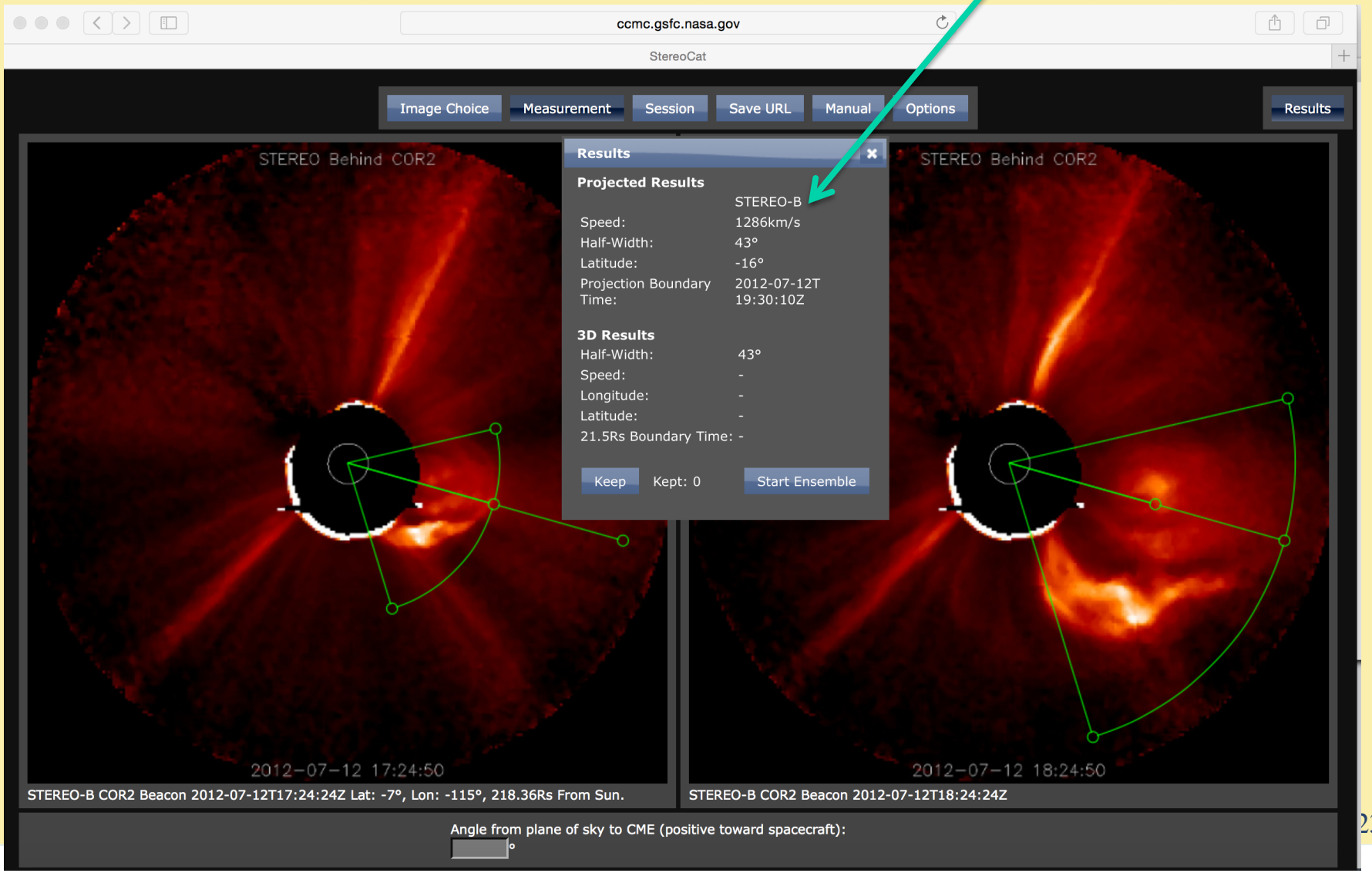

StereoCAT finds CME Start time

- CME start time = Snapshot Time – D/(CME speed) = 13:51

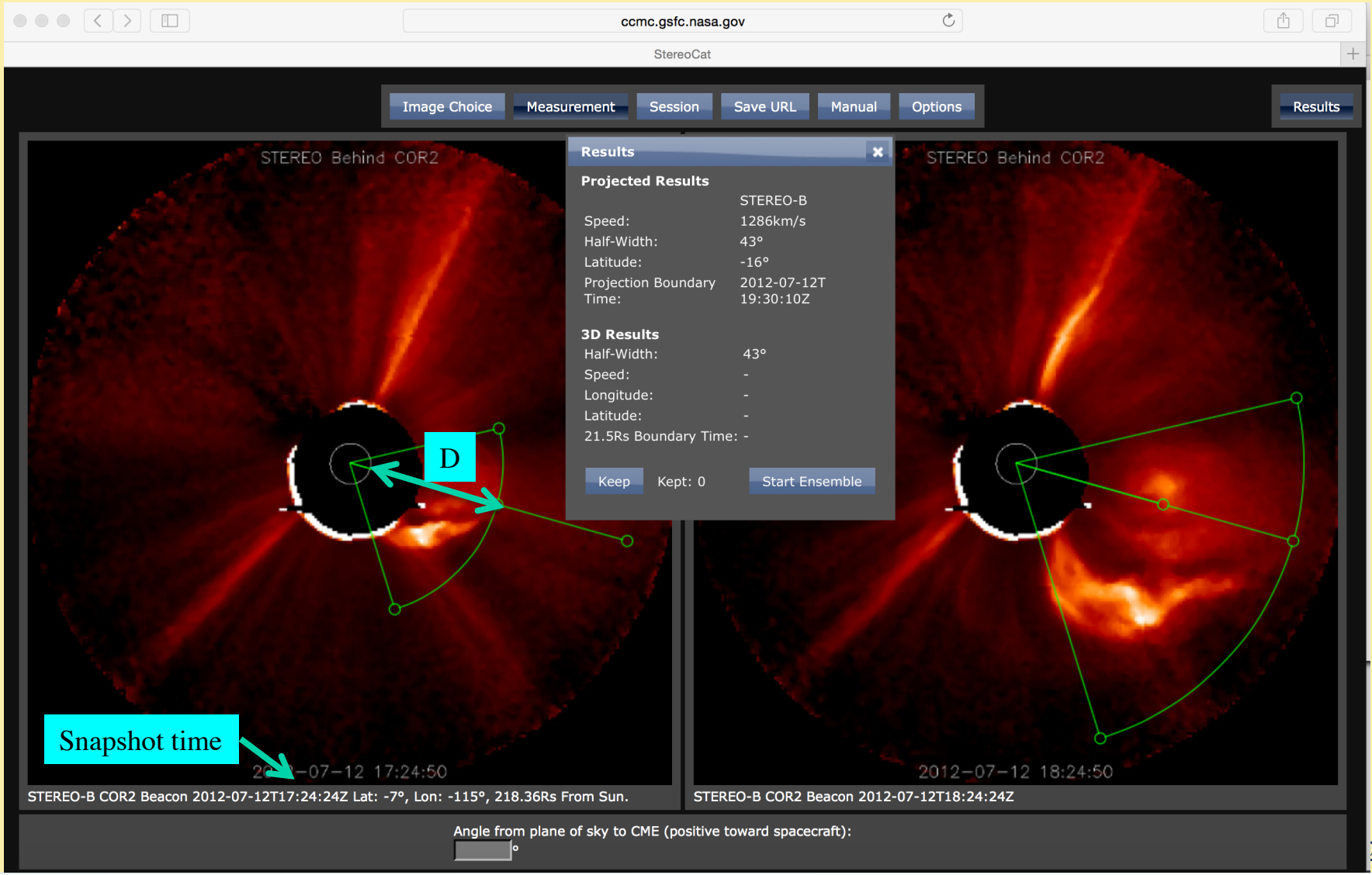

StereoCAT guesses CME place of birth

- Latitude is -20º. Estimates for (HEEQ) longitude are +/- 6º

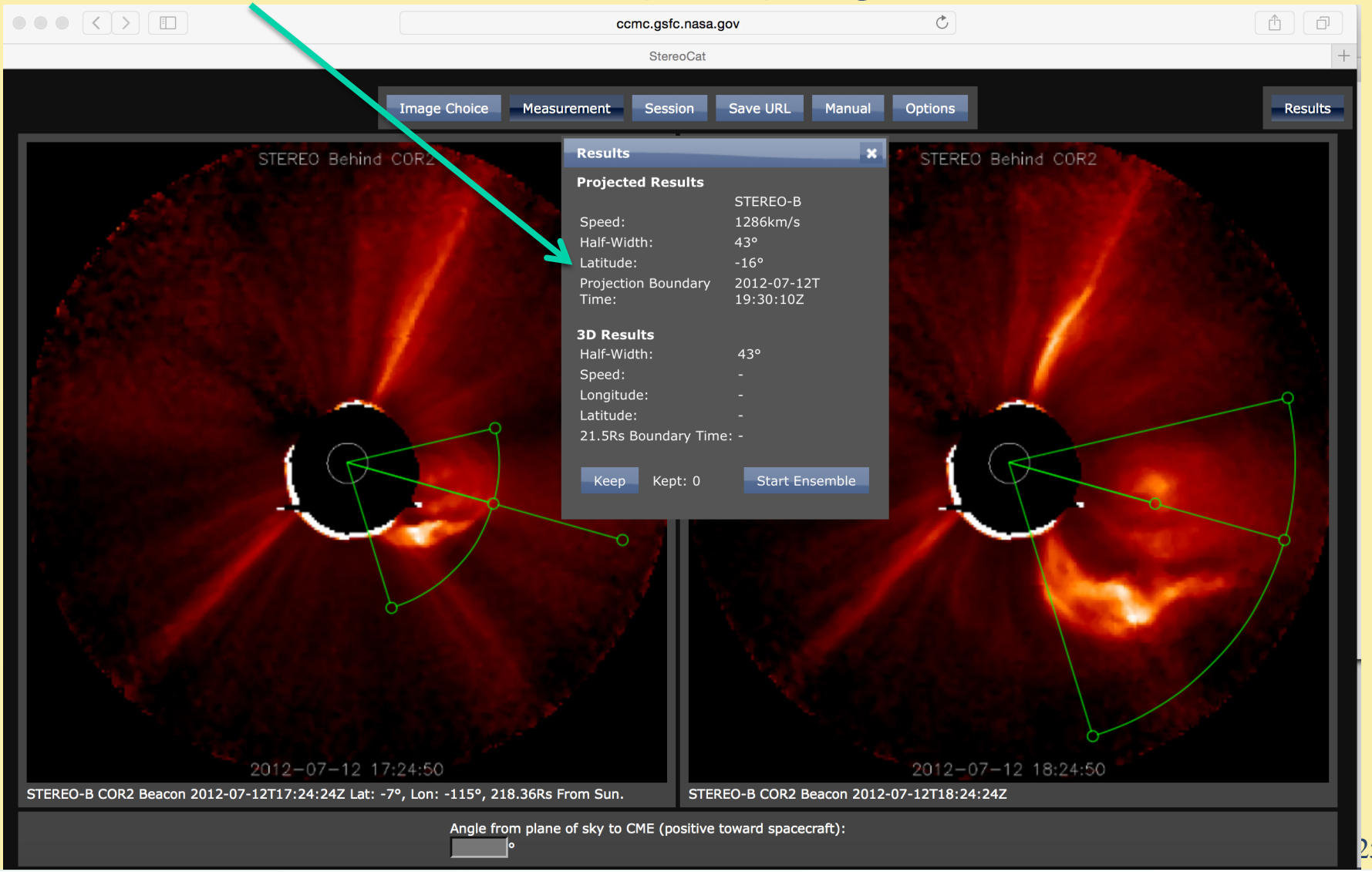

Newly Developed EEGGL tool

- **The new tool, EEGGL (Eruptive Event Generator using Gibson-Low configuration – see Splash page http://ccmc.gsfc.nasa.gov/analysis/EEGGLInfo/EEGGL.html**

  and the tool itself: http://ccmc.gsfc.nasa.gov/analysis/EEGGL/) has been recently developed at the CCMC (Goddard Space Flight Center) in collaboration with the University of Michigan.

- **Based on the magnetogram and evaluation of the CME initial location, speed, and start time the user may**
  - choose the active region from which the CME originates;
  - then the EEGGL tools provides the parameters of the Gibson-Low magnetic configuration to parameterize the CME;
  - the recommended parameters may be used then to drive the CME propagation from the low solar corona to 1 AU using the global code for simulating the solar corona and inner heliosphere. To achieve this, the EEGGL has a link to the run submission web page, which helps the user to fill in the request form for a simulation run.

EEGGL tool (historic events): chose AR

- For a start time, 2012-07-12.13:51 calculate CR number 2125 and Carrington longitude 83. Find AR in the synoptic magnetic map for CR2125 near the point with longitude 83+/-6^{o} and latitude -20^{0}

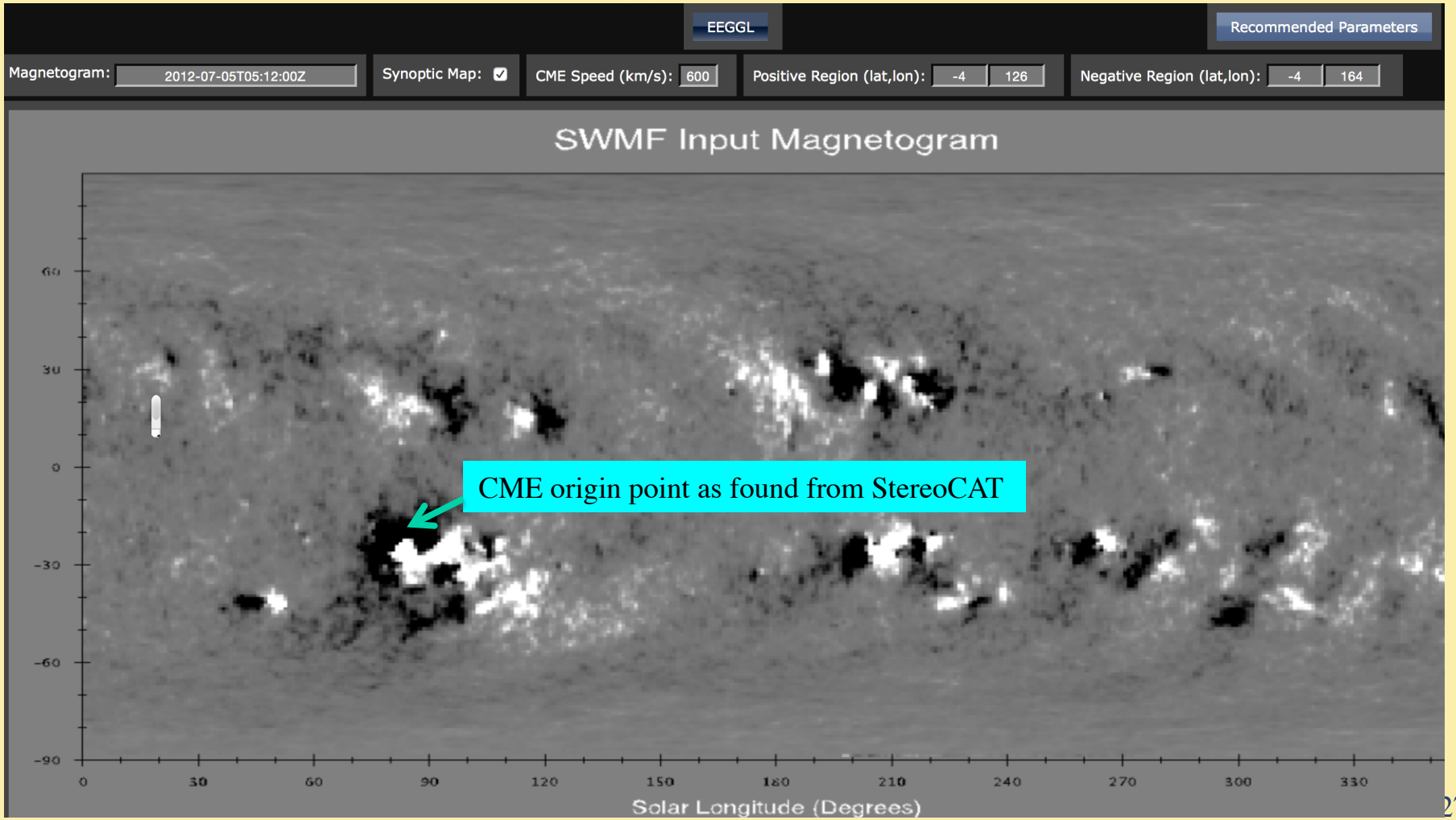

Find Parameters for GL configuration

- Choose and mark bipolar configuration of solar spots in this AR

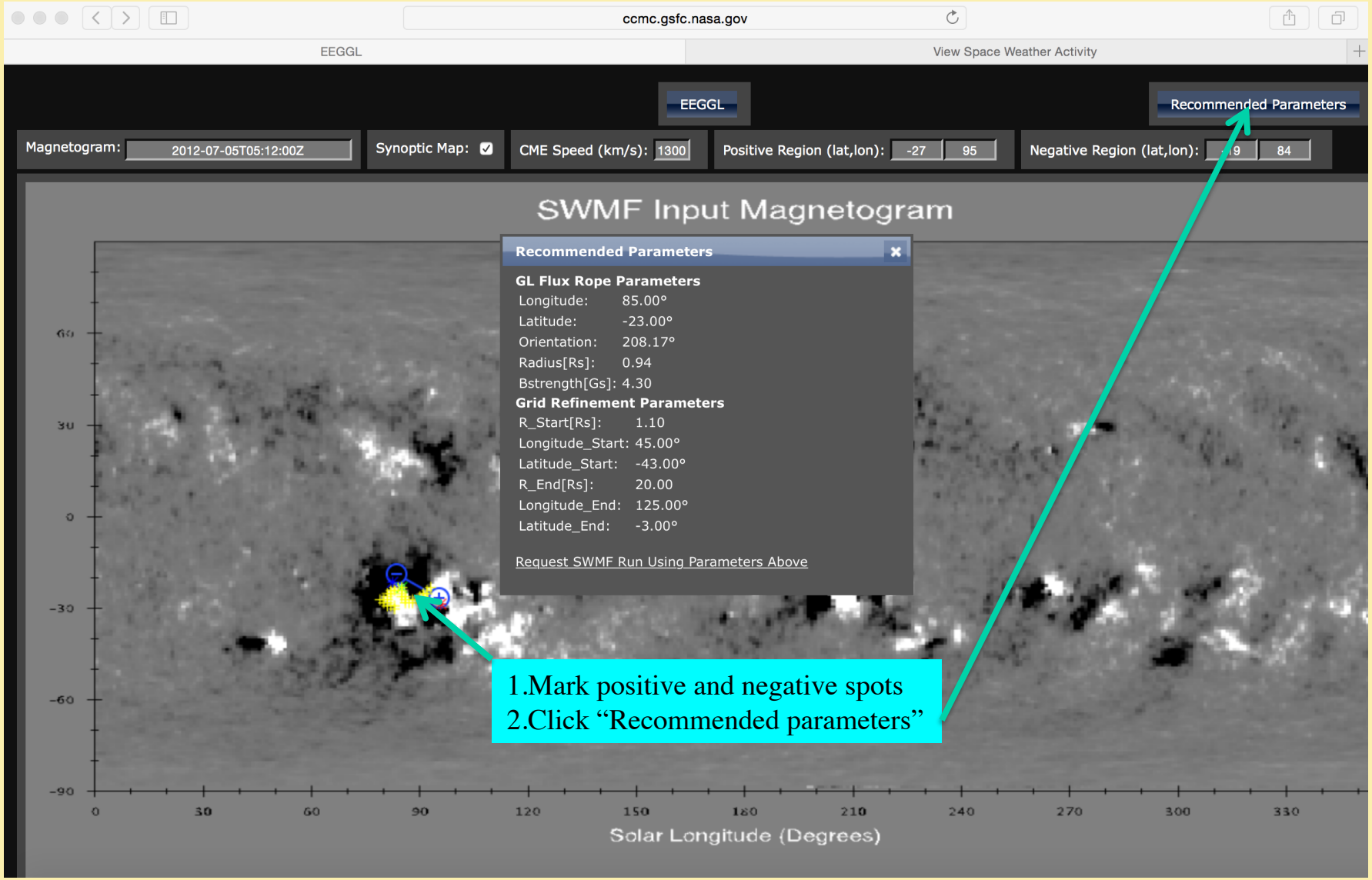

Fill in Form to Request Simulation Run

- With the found parameters for GL configuration request a run.

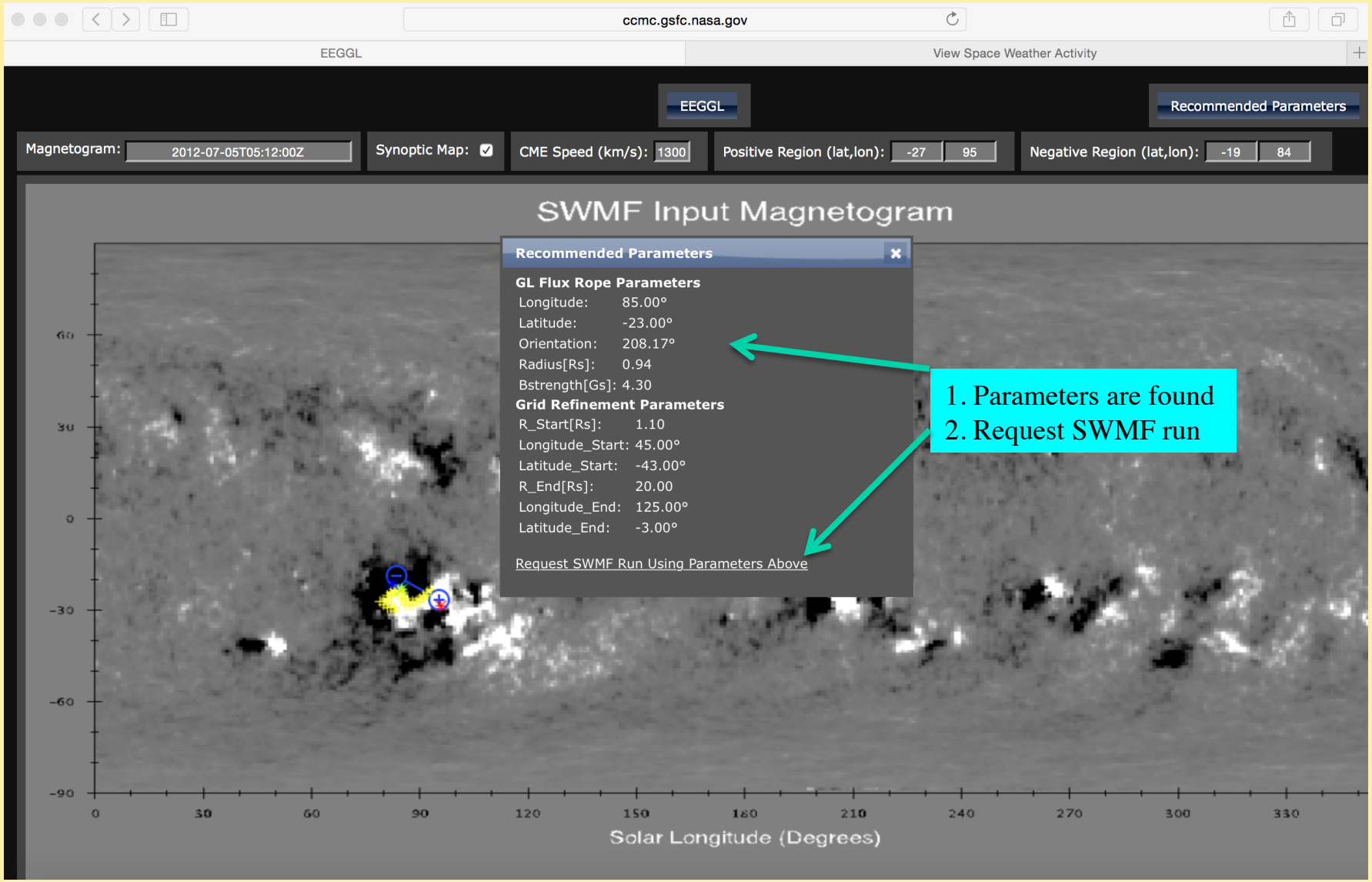

Submit Your Run and Wait

ccmc.gsfc.nasa.gov

SWMF AWSoM_R run submission | View Space Weather Activity

-START TIME-

Year:	2012
Mon:	07
Day:	12
Hour:	13
Min:	51

-GL FLUX ROPE PARAMETERS-

Longitude:	85
Latitude:	-23
Orientation:	208.17
Radius:	0.94
B Strength:	4.30

-Cone Opening Angle-

Longitude:	40
Latitude:	20
Special Request:	

BACK CONFIRM

Future Work

- We will add a capability to simulate real-time CMEs based on the existing automated real-time simulation system .

Acknowledgement

- The collaboration between the CCMC and University of Michigan is supported by the NSF SHINE grant 1257519 (PI Aleksandre Taktakishvili). The work performed at the University of Michigan was partially supported by National Science Foundation grants AGS-1322543 and PHY-1513379, NASA grant NNX13AG25G, the European Union's Horizon 2020 research and innovation program under grant agreement No 637302 PROGRESS. We would also like to acknowledge high-performance computing support from: (1) Yellowstone (ark:/85065/d7wd3xhc) provided by NCAR's Computational and Information Systems Laboratory, sponsored by the National Science Foundation, and (2) Pleiades operated by NASA's Advanced Supercomputing Division